Chinese Journal of Electronics
Vol.32, No.4, July 2023

Dual Radial-Resonant Wide Beamwidth Circular Sector Microstrip Patch Antennas

MAO Xiaohui[1], LU Wenjun[1,2], JI Feiyan[1], XING Xiuqiong[1], and ZHU Lei[3]

(1. *Jiangsu Key Laboratory of Wireless Communications, Nanjing University of Posts and Telecommunications, Nanjing 210003, China*)

(2. *Key Laboratory of Wireless Sensor Network & Communication, Shanghai Institute of Microsystem and Information Technology, Chinese Academy of Sciences, Shanghai 200050, China*)

(3. *Department of Electrical and Computer Engineering, Faculty of Science and Technology, University of Macau, Macau SAR, China*)

Abstract — In this article, a design approach to a radial-resonant wide beamwidth circular sector patch antenna is advanced. As properly evolved from a U-shaped d ipole, a prototype magnetic dipole can be fit in the radial direction of a circular sector patch radiator, with its length set as the positive odd-integer multiples of one-quarter wavelength. In this way, multiple $TM_{0m}(m = 1, 2, ...)$ modes resonant circular sector patch antenna with short-circuited circumference and widened E-plane beamwidth can be realized by proper excitation and perturbations. Prototype antennas are then designed and fabricated to validate the design approach. Experimental results reveal that the E-plane beamwidth of a dual-resonant antenna fabricated on air/Teflon substrate can be effectively broadened to 128°/120°, with an impedance bandwidth of 17.4%/7.1%, respectively. In both cases, the antenna heights are strictly limited to no more than 0.03-guided wavelength. It is evidently validated that the proposed approach can effectively enhance the operational bandwidth and beamwidth of a microstrip patch antenna while maintaining its inherent low profile merit.

Key words — Dual-resonant, Microstrip patch antenna, Radial-resonant modes, Wide beamwidth antenna.

I. Introduction

Wide beamwidth microstrip patch antennas (MPAs) are often highly demanded for various applications, such as wireless communication, broadcasting, and navigation [1]–[3]. Ordinary microstrip square patch antennas suffer from limited half-power beamwidths (HPBWs), which are usually 60° [4]. In the past few decades, various techniques have been developed to broaden HPBWs of MPAs. These approaches can be basically divided into five distinct types in terms of their operation principles. As the most common way, the reflector-shaping method is presented in references [5]–[12]: Herein, the size and shape of a ground plane is employed to control the radiation characteristics of MPAs [9]. MPAs with different-shaped reflectors, such as square and tapered-elliptical cavity [5]–[8], cylindrical [9], [10] and tapered reflectors [11], can realize a much wider HPBW than their ordinary ones, at the cost of higher antenna height. To maintain the inherent low-profile merit, the following four methods have been proposed. The first one is the use of rotational elements [13]–[16]. As seen, a low-profile backed cavity with crossed slits can yield a widened beamwidth [13]. With identical elements being symmetrically rotated to form an array, a wide beamwidth characteristic can alternatively be obtained [14]–[16]. The second type is to use the complementary dipole technique [17]–[20], e.g., combination of magnetic dipole and electric dipole toward stable unidirectional patterns with wide beamwidth [17]. The third way is the use of parasitic elements [21]–[25]. Parasitic elements such as L-probe [21], mushroom-shaped patch [22], metallic wall [23], [24], and shorting-pin [25] are included to design a wide beamwidth antenna. The final one is the material-based technique [26]–[30]. Meta-materials such as polarization

Manuscript Received June 25, 2021; Accepted Mar. 20, 2022. This work was supported by the National Natural Science Foundation of China (61871233), the Research Project of Key Laboratory of Wireless Sensor Network & Communication, the Shanghai Institute of Microsystem and Information Technology (20200604), and the Postgraduate Research & Practice Innovation Program of Jiangsu Province (KYCX20_0808).

 DOI:10.23919/cje.2021.00.219

rotation reflective surface [26], reactive impedance surface (RIS) [27], electromagnetic band gap structure [28] and frequency-selective surface (FSS) [30] can be effectively used as various beamwidth broadening techniques. Recently, a few innovative approaches based on self-balanced theory [31] and capacitive via fence [32], [33] have been advanced. Unfortunately, the planar self-balanced technology is strongly dependent on the size and shape of the ground plane of the antenna [31], and the blind bolt technique may incorporate geometrical complexity and narrow-band operation [32], [33]. Therefore, it is always a challenging task to develop a wide beamwidth antenna with simple structure, wideband operation, and low profile (i.e., height less than 0.1-guided wavelength) characteristics.

This article advances a novel design approach to dual radial-resonant, wide beamwidth, circular sector patch antenna. Firstly, the operation principle of radial-resonant patch antenna evolved from a U-shaped dipole is intuitively revealed. Then, key parameters are initially determined by mode synthesis table and dual radial-resonant, circular sector patch antennas with short-circuited circumference can be designed accordingly. Finally, the radial-resonant design approach is experimentally verified by prototype antennas fabricated on air and Teflon substrates.

II. Theory and Design Approach

The radial-resonant circular sector patch antenna with short-circuited circumference is presented here with widened E-plane beamwidth, and it is basically evolved from a simplest, U-shaped dipole antenna with quasi-isotropic radiation pattern [34], as shown in Fig.1. Then, a mode synthesis method of patch antenna is revealed, and the key design parameters can accordingly be calculated and determined.

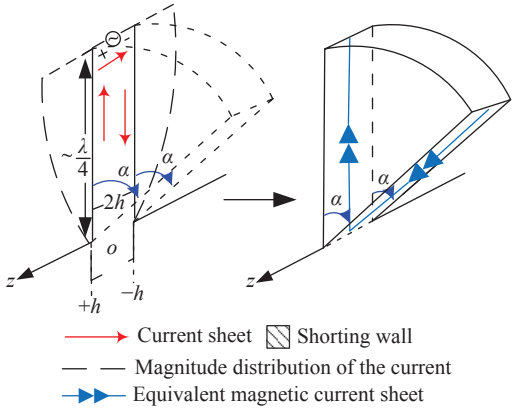

Fig. 1. Evolution of the proposed radial-resonant antenna.

1. Evolution from a horizontal U-shaped dipole

The evolution of the proposed antenna is depicted in Fig.1. A horizontal, one quarter-wavelength, U-shaped dipole is used as the original prototype. The open aperture of the dipole coincides to the z-axis. By rotating the horizontal arms and short cross piece to a certain angle of α, the prototype 1-D dipole can evolve into a 2-D circular sector cavity with short-circuited circumference, where its height is denoted as $2h$. Equivalently, the evolved antenna can be recognized as a circumferentially short-circuited, circular sector antenna with flared angle of α, height of h and infinite ground plane according to the theory of image: As such, the antenna should only exhibit magnetic current distribution in the radial direction as shown in Fig.1.

The short-circuited circumference implies that the circumferential eigen-number must be zero, and the magnetic current should have only ρ component that obeying the zero-order Bessel equation. By inserting the asymmetric boundary conditions at $\rho = 0,\ R_0$ into (1), the general solution can be attained to dominate the eigen-modes, where R_0 is the radius of circular sector patch, A is an arbitrary, undetermined coefficient.

$$\left.\begin{array}{l}\left(\rho^2\dfrac{d^2}{d^2\rho}+\rho\dfrac{d}{d\rho}+k_\rho^2\right)M(\rho)=0\\ M|_{\rho=R_0}=0\\ \dfrac{\partial M}{\partial\rho}|_{\rho=0}=0\end{array}\right\}\Rightarrow M(\rho)=AJ_0(k_\rho\rho) \tag{1}$$

2. Dual-resonant design approach

The normalized radius of the patch can be estimated by the length of the equivalent magnetic dipole and the roots of the zero-order Bessel function [35], [36]: On one hand, according to the asymmetric boundary condition at $\rho = 0,\ R_0$ (i.e., $\rho = R_0,\ M = 0$; and $\rho = 0,\ \partial M/\partial\rho = 0$), the length of the prototype magnetic dipole should thus satisfy $L = 2R_0 = n\lambda_0/4$, as shown in (2a), where L is the length of equivalent magnetic dipole [37]. The radius of the cavity model can be estimated by (2b). In the single-mode resonant case [38], the normalized radius can be calculated by (3). In the dual-resonant case, the radius of the circular sector patch can be alternatively estimated by (4) [37].

$$L=\frac{n\lambda_0}{4}=2R_0,\quad n=1,3,5,\ldots \tag{2a}$$

$$2R_0=\frac{\chi_{0,m}}{\pi}\lambda_0,\quad m=1,2,3,\ldots \tag{2b}$$

$$\begin{cases}2\bar{R}_0=\dfrac{L}{\lambda_0}=\dfrac{n}{4}, & n=1,3,5,\ldots\\ 2\bar{R}_0=\dfrac{\chi_{0,m}}{\pi}, & m=1,2,3,\ldots\end{cases} \tag{3}$$

$$2\bar{R}_0=\frac{\chi_{0,1}+\chi_{0,2}}{2\pi} \tag{4}$$

Using (3) and (4), a mode synthesis table (Table 1) can be attained. When $m = 1$, the difference between line 2 and line 4 of Table 1 is 0.01, which corresponds to the single, fundamental TM_{01} mode resonant case [38]. Values in line 3 and line 7 of Table 1 can be approximately regarded as equal with difference of 0.01. It can be figured out that a dual, TM_{01}/TM_{02} mode resonance can be excited in $L = 2R_0 = 1.25\lambda_0$ case.

Table 1. Mode synthesis of the conceptual radial-resonant circular sector patch antennas

$2\bar{R}_0 = \frac{n}{4}$	$n = 1$	0.25
	$\boldsymbol{n = 3}$	**0.75**
	$\boldsymbol{n = 5}$	**1.25**
$2\bar{R}_0 = \frac{\chi_{0,m}}{\pi}$	$\boldsymbol{m = 1}$	**0.76**
	$m = 2$	1.76
	$m = 3$	2.75
$2\bar{R}_0 = \frac{\chi_{0,1} + \chi_{0,2}}{2\pi}$		**1.26**

In order to maintain a pure radial-mode resonance and suppress the circumferential ones, circumference of the circular sector patch ($R_0\alpha$) should be less than the length of prototype magnetic dipole ($L = 2R_0$), thus the flared angle α should be satisfied with

$$\left.\begin{array}{l} R_0\alpha \le L \\ L = 2R_0 \end{array}\right\} \Rightarrow \alpha \le 2 \tag{5}$$

Therefore, the flared angle α of the radial-resonant circular sector patch antenna should be no more than 115° (i.e., 2-radian). In practical engineering design, such constraint can be slightly modified to $\alpha \le 120°$.

Fig.2 qualitatively illustrates the surface electric, magnetic current density and Electric-field distributions of the first two radial-resonant modes (TM_{01} and TM_{02} modes) within a conceptual microstrip circular sector radiator with short-circuited circumference.

As shown in Fig.2, a nodal line exhibits on the patch surface and its position R_s can be determined by

$$\frac{R_s}{R_0} = \frac{\chi_{0,1}}{\chi_{0,2}} \approx 0.43 \tag{6}$$

In order to disturb the TM_{02} mode properly, twin arc slits with length L_s and width W_s are introduced at R_s [39]. According to the empirical equations [40], the length L_s and the width W_s of slits can be determined by (7) and (8)

$$L_s \approx \frac{\lambda_H}{4} = \frac{\chi_{0,1}c}{2(\chi_{0,1} + \chi_{0,2})f_0} \tag{7}$$

$$W_s \approx \frac{\lambda_H}{20} = \frac{\chi_{0,1}c}{10(\chi_{0,1} + \chi_{0,2})f_0} \tag{8}$$

where λ_H is the corresponding wavelength of the high

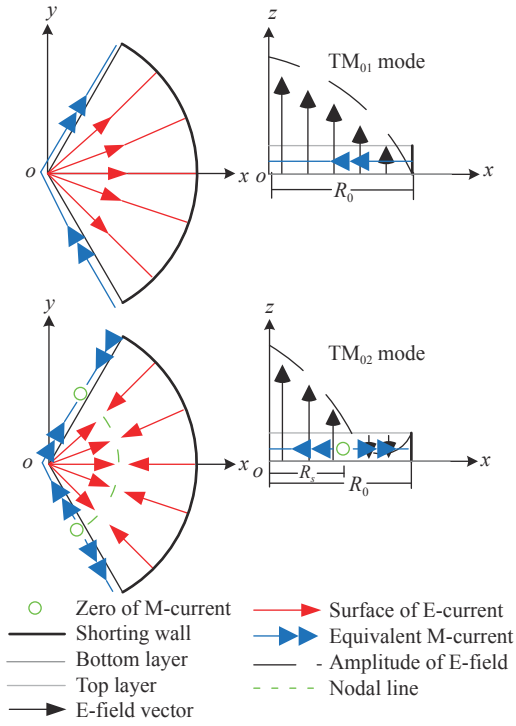

Fig. 2. Radial surface electric/magnetic current density distributions and cross-sectional electric-fields of TM_{01} and TM_{02} modes within a circular sector radiator.

order resonant mode. Therefore, when the center frequency is 3.6 GHz, the radius of the circular sector patch should be approximately determined as $R_0 = 52.4$ mm. Thus, the initial value of slits can be approximately set as $L_s = 12.6$ mm and $W_s = 2.5$ mm.

A shorting pin is introduced between the feed and the shorting wall, aiming to perturb radial-resonant modes and attain dual-mode resonance [41]. Empirically, the distance between the pin and the center of the circular sector can be set as one-fourth to one-third of the patch radius [42], [43], thus the shorting pin should be set at $(x_1, 0) = (17.5$ mm, $0)$. Based on this analysis, most of design parameters can be initially determined. Hence, the dual radial-resonant circular sector patch antenna is resulted as shown in Fig.3, and parametric studies are then performed as shown in Fig.4.

In simulation, better impedance is obtained by placing the feeding probe at $(x_0, 0) = (12.5$ mm, $0)$ [4], [44] and $\alpha = 90°$. In addition, the radius of the ground plane is set as $R_g = 70.0$ mm, which is larger than one half-wavelength. As shown in Fig.4(a), TM_{01} and TM_{02} modes can be simultaneously excited at 2.3 and 4.85 GHz in the unloaded case. When a pin is loaded, both TM_{01} mode and TM_{02} mode can be perturbed and tuned upward to 3.52 and 5.02 GHz. When slits are incorporated at the nodal line position, TM_{02} mode can be tuned down to 3.91 GHz. When both pin and slits are incorporated, dual radial-resonant characteristic can

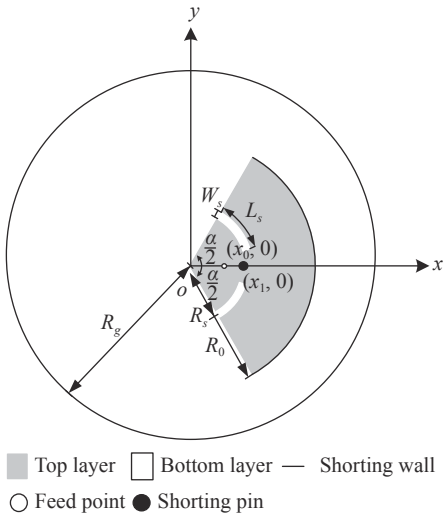

Fig. 3. Geometry of the proposed dual radial-resonant antenna.

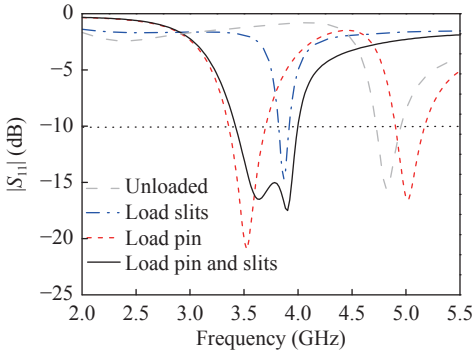

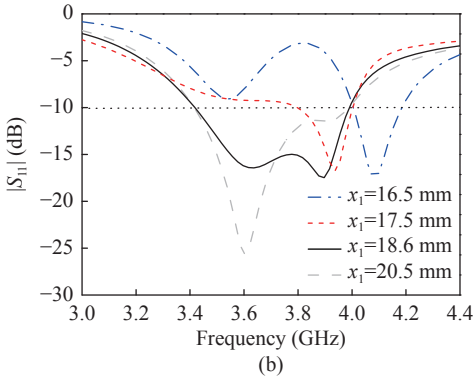

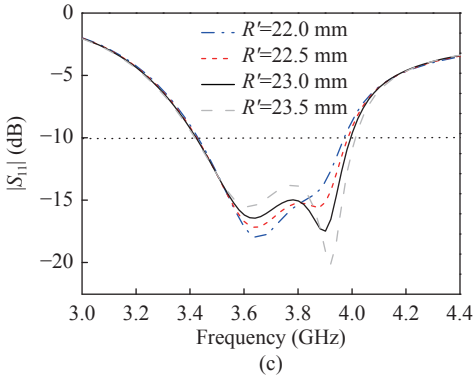

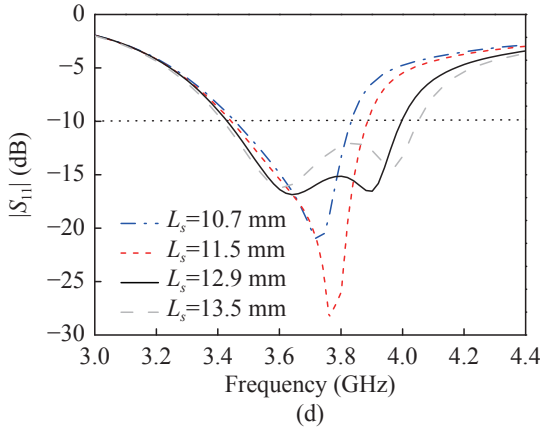

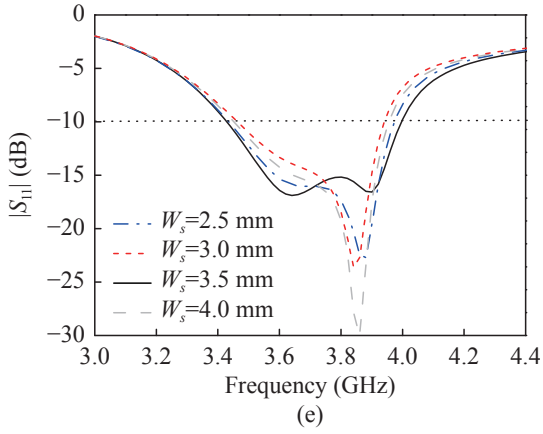

Fig. 4. Parametric studies on the pin, slits and the position of pin and slits. (a) Reflection coefficients: comparison between unloaded, load pin, load slits and load pin and slits cases; (b) x_1 (R_s = 23.0 mm, L_s = 12.9 mm, W_s = 2.5 mm); (c) R_s (x_1 = 18.6 mm, L_s = 12.9 mm, W_s = 2.5 mm); (d) L_s (x_1 = 18.6 mm, R_s = 23.0 mm, W_s = 2.5 mm); and (e) W_s (x_1 = 18.6 mm, R_s = 23.0 mm, L_s = 12.9 mm).

be yielded at 3.6 GHz band. In Fig.4(b), both TM_{01} and TM_{02} modes are sensitive to the position of the pin. Fig.4(c) and Fig.4(e) indicate that the position and the width of slits have little effect on the two resonant frequencies, but play important roles in impedance matching. Therefore, wider bandwidth can be obtained by properly adjusting the position and width of those slits. As can be seen from Fig.4(d), the length of slits should be a critical parameter for impedance matching, so it should be finely tuned according to formula (7). Based on the above step-by-step numerical studies, the final key parameters can be determined, compared and tabulated in Table 2. It is found that the theoretical and simulated results agree well with each other, with discrepancy less than 6.5%. The correctness and effectiveness of the design approach have been thus numerically validated.

3. Experiment validations

Further experimental validations of the dual radial-resonant design approach are performed herein. Fig.5

Table 2. Key parameters of the dual-mode antenna (unit: mm)

Parameter	Theoretical	Simulated
R_0	52.4	52.4
R_s	22.5	23.0
L_s	12.6	12.9
W_s	2.5	2.5
x_1	17.5	18.6
R_g	70.0	
x_0	12.5	

shows the photograph of the fabricated dual radial-resonant antenna on air substrate with height $h = 3.0$ mm. As shown in Fig.6, the measured central frequency is 3.72 GHz and it matches well with the simulated one with a discrepancy less than 0.1%. The measured -10 dB reflection coefficient bandwidth is 17.4% in a range from 3.4 to 4.05 GHz, and the simulated one is 15.3% in a range from 3.43 to 3.99 GHz. It is obvious that the antenna under dual radial-resonant operation exhibits a tripled wider impedance bandwidth than that of a conventional circular patch antenna (approximately 6.0%) [4].

Fig. 5. Photograph of the fabricated dual-mode antenna on air substrate.

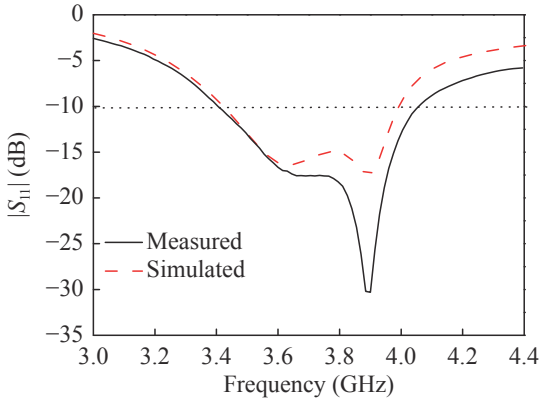

Fig. 6. Simulated and measured reflection coefficients of a dual-mode antenna designed on air substrate.

Fig.7 presents the simulated electric field at 3.63 and 3.9 GHz. As compared to the theoretical analysis in Fig.2, it can be seen that the proposed antenna should operate under TM_{01} and TM_{02} modes at 3.63 and 3.9 GHz. It indicates that the two radial-resonant modes are simultaneously excited under dual-mode resonance. The successful dual-mode excitation reveals the correctness of the dual radial-resonant design approach.

Fig.8 demonstrates the measured radiation patterns with the simulated ones in zx-plane and zy-plane at $f = 3.63$, 3.78 and 3.9 GHz. As seen, measured and simulated radiation patterns all match well with each other. At $f = 3.63$, 3.78 and 3.9 GHz, the antenna exhibits measured beamwidths of 128°/72°, 122°/66° and 107°/52° in zx-plane and zy-plane, respectively. As such, the proposed antennas can exhibit a stable, wide E-plane beamwidth within impedance bandwidth.

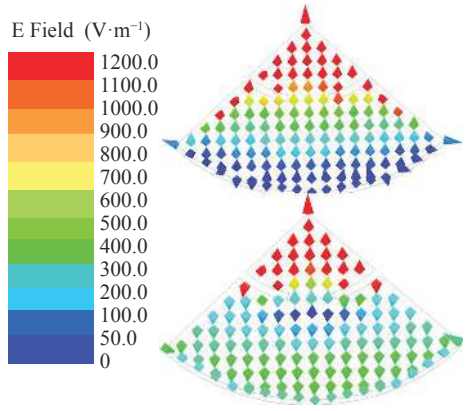

Fig. 7. Simulated E-field distributions at 3.63 GHz and 3.9 GHz.

As shown in Fig.8, due to the fully-excited TM_{02} mode, the radiation patterns present slight tilt beams with peak gain occurred at $\theta = \pm 45°$. Fortunately, the difference between the measured peak and bore-sight gains is smaller than 2 dB, and the in-band bore-sight gain varies less than 3 dB. The measured average radiation efficiency within impedance bandwidth is about 87.9% and it matches well with the simulated one, as shown in Fig.9. These results validate the dual radial-resonant approach to wide beamwidth, circumferentially short-circuited circular sector patch antenna to be correct and effective.

Fig.10 shows a printed prototype on a modified Teflon substrate with $h = 2.0$ mm and $\epsilon_r = 2.65$, aiming at further verifying the dual-resonant design approach's versatility. Refer to the case of air substrate, the key parameters of the fabricated antenna can be adjusted to $R_0 = 35.3$ mm, $R_g = 50.0$ mm, $R_s = 17.4$ mm, $x_0 = 5.0$ mm, $x_1 = 18.0$ mm, $L_s = 12.5$ mm, and $W_s = 2.1$ mm [4].

Fig.11 shows the reflection coefficients of the antenna (simulated and measured) and a reference, circular patch antenna (simulated only) on the same substrate. The center frequency is designed at 3.65 GHz, where a slight discrepancy between the measured and simulated ones is about 0.4%. The fabricated antenna exhibits a dual-resonant characteristic as its simulated counterpart and measured impedance bandwidth (for $|S_{11}| < -10$ dB) is 7.1% covering a range from 3.54 to 3.8 GHz, while the simulated one of the reference an-

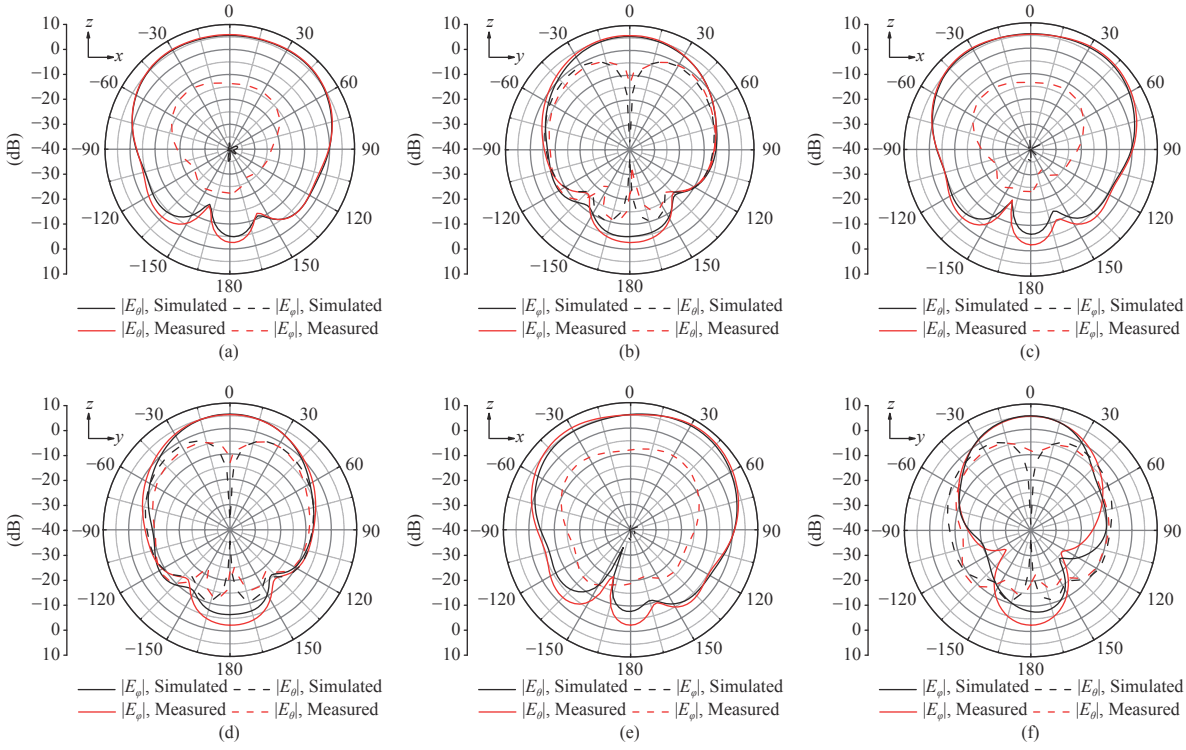

Fig. 8. Simulated and measured radiation patterns in zx- and zy-plane at different frequencies. (a) and (b) at 3.63 GHz; (c) and (d) at 3.78 GHz; (e) and (f) at 3.9 GHz.

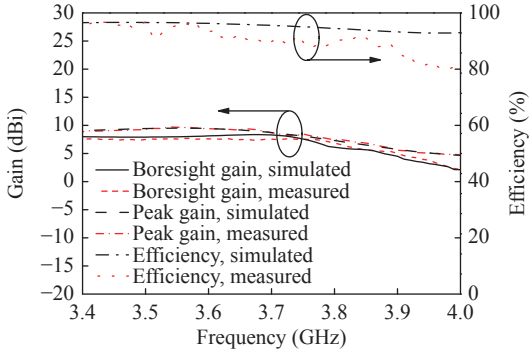

Fig. 9. Simulated and measured radiation gains and efficiencies.

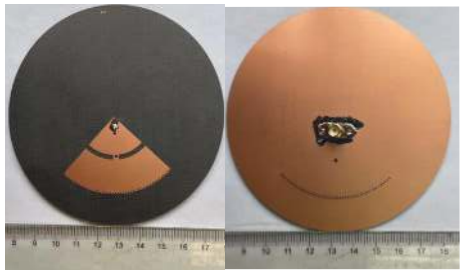

Fig. 10. Photograph of the printed patch antenna prototype on modified Teflon substrate.

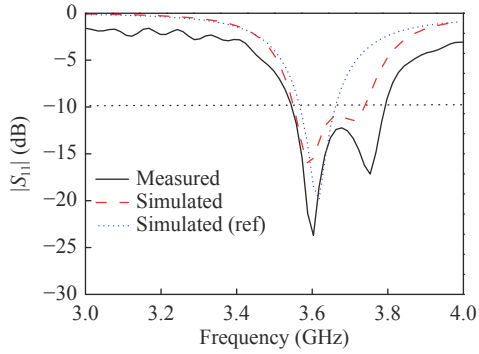

Fig. 11. Simulated and measured reflection coefficients of dual radial-resonant antenna designed on modified Teflon substrate.

tenna is 2.3% only. Therefore, the advanced dual radial-resonant design approach should be effective for printed antennas, too.

Fig.12 depicts the simulated and measured radiation patterns of the printed antenna in zx- and zy-plane at f = 3.55, 3.65, and 3.75 GHz. All measured and simulated patterns are in good agreement with each other, as shown in Fig.12. Wide beamwidths can be found in Fig.12(a), (c), and (e). The measured E-plane beamwidths are 117°, 100° and 120° at f = 3.55, 3.65, and 3.75 GHz, respectively. In H-plane, the corresponding beamwidths are 77°, 68° and 58°. As TM_{02} mode is fully excited, the radiation patterns at all frequencies are slightly titled but still hold stable broadside radiation patterns as like its air-substrate counterpart.

Fig.13 shows the radiation efficiencies, bore-sight gains and peak gains of the proposed printed dual radial-resonant antenna. Within the impedance bandwidth, both measured and simulated bore-sight gains exhibit a

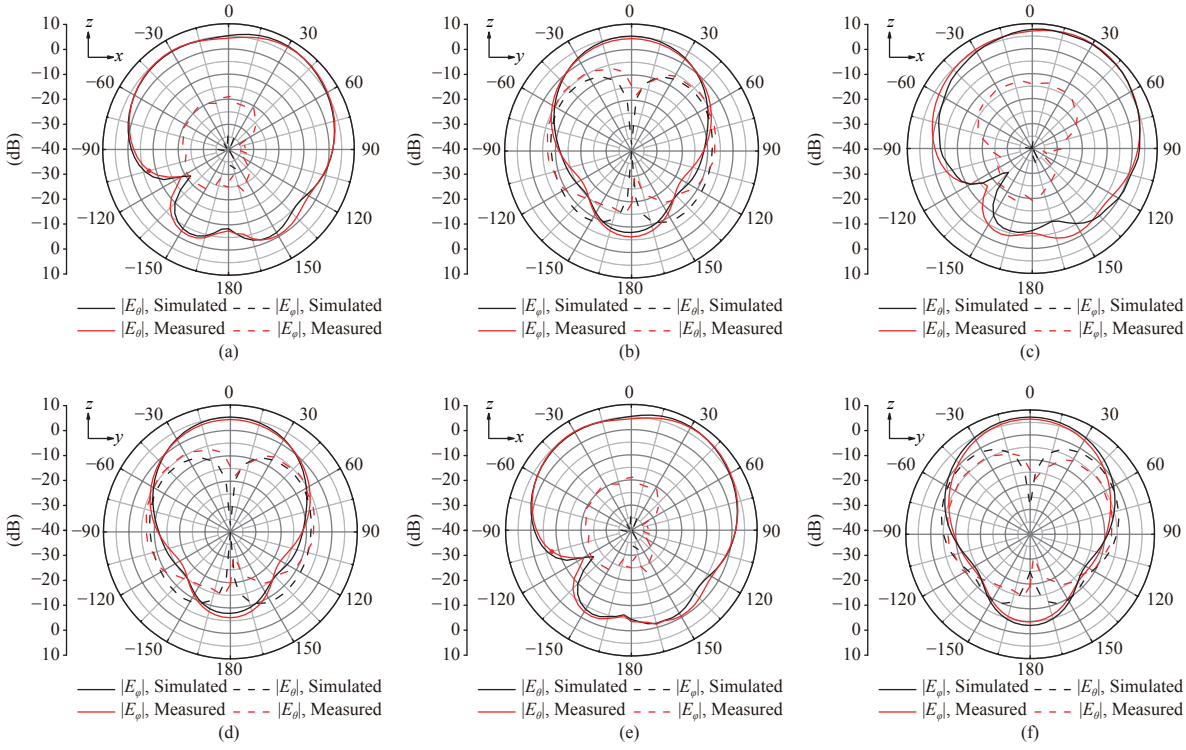

Fig. 12. Simulated and measured radiation patterns in zx- and zy-plane at different frequencies. (a) and (b) at 3.55 GHz; (c) and (d) at 3.65 GHz; (e) and (f) at 3.75 GHz.

stable characteristic with a minor fluctuation less than 3.0 dB and the maximum measured one can reach to 7.3 dBi. Similar to the air-substrate case, although the peak gain deviates slightly from the $+z$-direction, the differences between the peak gains and the bore-sight gains are less than 3.0 dB. In addition, as its air-substrate counterpart behaves, the measured and simulated efficiencies agree well with each other and the measured in-band average efficiency is up to 85.7%. Again, these results convince the correctness and effectiveness of the advanced design approach.

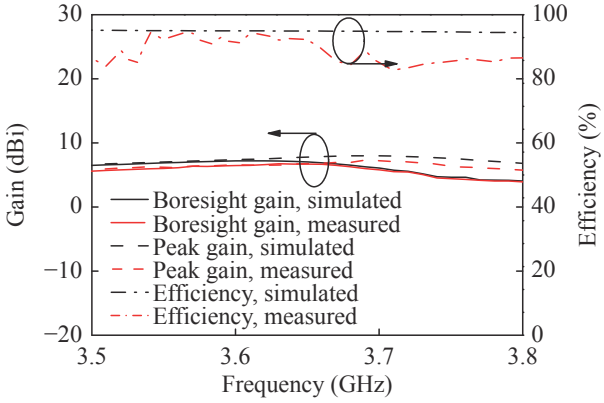

Fig. 13. Simulated and measured radiation gains and efficiencies.

III. Comparisons and Discussions

Table 3 presents systematical comparisons between the proposed antennas and the latest counterparts in the aspects of operation principle, impedance bandwidth, patch electrical size, HPBW in E-plane, complexity (number of design parameters) and operational mode. Compared to its counterparts, the proposed antennas exhibit the lowest configuration complexity with only 6 key design parameters and an extremely low profile, which makes the proposed one more promising to conformal design [21]–[46]. Compared to the wideband counterparts [21], [31], the advanced antenna have a wider beamwidth, and can be flexibly implemented on the ultra-slim substrate. Compared to the designs with identical height and wider bandwidth [24], the advanced antenna can exhibit a more compact size of less than 1.0-wavelength. Such merit makes the advanced antenna more useful for array designs than its counterpart [24]. Comparing to the low-profile designs in [32], [33], the advanced antenna's bandwidth is nearly tripled to the counterparts'. In addition, the proposed antennas can be easily implemented and fabricated without introducing additional cavity [25], multiple elements [32], or special blind bolt fence [33]. Compared with the self-balanced counterparts [31], [45], the proposed antennas are independent to the size and shape of the ground plane and more suitable for various applications mounted above a bulky ground plane. Besides, the wider impedance bandwidth and HPBW can also be obtained by adjusting the flared angle α or cooperating with other

Table 3. Wide beamwidth magnetic-type antennas for comparisons (N.A. =Not Available)

References	Principle of operation	Impedance bandwidth	Patch electrical size	HPBWs E-plane	Number of design parameters	Operational modes
[21]	Parasitic elements	34.8%	$0.9\lambda_g \times 0.9\lambda_g \times 0.4\lambda_g$	101°	13	N.A.
[24]	Parasitic elements	12.0%	$0.45\lambda_g \times 1.02\lambda_g \times 0.029\lambda_g$	140°	11	TM_{10}/TM_{12}
[25]	Metallic cavity	9.9%	$0.49\lambda_g \times 0.49\lambda_g \times 0.07\lambda_g$	116°	7	N.A.
[31]	Self-balanced magnetic dipole	20.0%	$0.29\lambda_g \times 0.049\lambda_g$	90°–100°	6	$TM_{11}/TM_{3/4,1}$
[32]	Parasitic elements	2.7%	$0.52\lambda_g \times 0.52\lambda_g \times 0.03\lambda_g$	132°	8	TM_{11}
[33]	Blind bolt fence	3.0%	$0.19\lambda_g \times 0.19\lambda_g \times 0.07\lambda_g$	107°	11	TM_{10}
[45]	Self-balanced magnetic dipole	16.0%	$0.29\lambda_g \times 0.049\lambda_g$	115°–130°	7	TM_{11}
[46]	Parasitic elements	13.4%	$1.15\lambda_g \times 4.95\lambda_g \times 0.1\lambda_g$	126°	16	N.A.
This work	Dual radial-resonant	17.4%/7.1%	$0.625\lambda_g \times 0.03\lambda_g$	100°–128°	6	TM_{01}/TM_{02}

methods. Therefore, the comparative results evidently prove the effectiveness and advantages of the radial-resonant design approaches.

IV. Conclusions

In this article, a novel design approach to radial-resonant MPAs has been systematically advanced. Dual TM_{0m} ($m = 1, 2$) modes resonant, wide beamwidth MPAs have been successfully designed and implemented on both air and dielectric substrates. As experimentally demonstrated, advanced antennas exhibit wide beamwidth characteristics within zx-plane (i.e., approximately 128°). Compared to existing design approaches, the advanced radial-resonant one can maintain the inherent low-profile characteristic of the MPAs, offer broader bandwidth and wider beamwidth, exhibit simpler configuration in geometry, etc. Therefore, the proposed design approaches would be promising in development of a variety of other low-profile wide beamwidth microstrip antennas in the future.

References

[1] K. Carver and J. Mink, "Microstrip antenna technology," *IEEE Transactions on Antennas and Propagation*, vol.29, no.1, pp.2–24, 1981.

[2] H. Wong, K. M. Luk, C. H. Chan, *et al.*, "Small antennas in wireless communications," *Proceedings of the IEEE*, vol.100, no.7, pp.2109–2121, 2012.

[3] K. F. Lee and K. F. Tong, "Microstrip patch antennas-basic characteristics and some recent advances," *Proceedings of the IEEE*, vol.100, no.7, pp.2169–2180, 2012.

[4] R. Garg, P. Bhartia, I. Bahl, *et al.*, *Microstrip Antenna Design Handbook*. Artech House, Boston, 2001.

[5] T. P. Wong and K. M. Luk, "A wide bandwidth and wide beamwidth CDMA/GSM base station antenna array with low backlobe radiation," *IEEE Transactions on Vehicular Technology*, vol.54, no.3, pp.903–909, 2005.

[6] X. Bai, S. W. Qu, S. W. Yang, *et al.*, "Millimeter-wave circularly polarized tapered-elliptical cavity antenna with wide axial-ratio beamwidth," *IEEE Transactions on Antennas and Propagation*, vol.64, no.2, pp.811–814, 2016.

[7] C. L. Tang, J. Y. Chiou, and K. L. Wong, "Beamwidth enhancement of a circularly polarized microstrip antenna mounted on a three-dimensional ground structure," *Microwave and Optical Technology Letters*, vol.32, no.2, pp.149–153, 2002.

[8] T. P. Wong and K. M. Luk, "Wideband and wide beamwidth L-probe patch antenna array with a novel ground plane for backlobe reduction," in *Proceedings of the IEEE Antennas and Propagation Society International Symposium. Digest. Held in Conjunction with: USNC/CNC/URSI North American Radio Sci. Meeting*, Columbus, OH, USA, pp.880–883, 2003.

[9] S. Noghanian and L. Shafai, "Control of microstrip antenna radiation characteristics by ground plane size and shape," *IEE Proceedings-Microwaves, Antennas and Propagation*, vol.145, no.3, pp.207–212, 1998.

[10] I. J. Nam, S. M. Lee, and D. Kim, "Advanced monopole antenna with a wide beamwidth for the assessment of outdoor 5G wireless communication environments," *Microwave and Optical Technology Letters*, vol.60, no.9, pp.2096–2101, 2018.

[11] D. Ling and G. Lu, "Wideband magneto-electric dipole antenna with stable wide E-plane beamwidth", in *Proceedings of 2018 IEEE 4th International Conference on Computer and Communications (ICCC)*, Chengdu, China, pp.1042–1046, 2018.

[12] K. S. Feng, N. Li, Q. W. Meng, *et al.*, "Study on dielectric resonator antenna with annular patch for high gain and large bandwidth," *Chinese Journal of Electronics*, vol.24, no.4, pp.869–872, 2015.

[13] D. Sievenpiper, H. P. Hsu, and R. M. Riley, "Low-profile cavity-backed crossed-slot antenna with a single-probe feed designed for 2.34-GHz satellite radio applications," *IEEE Transactions on Antennas and Propagation*, vol.52, no.3, pp.873–879, 2004.

[14] K. M. Mak and K. M. Luk, "A circularly polarized antenna with wide axial ratio beamwidth," *IEEE Transactions on Antennas and Propagation*, vol.57, no.10, pp.3309–3312, 2009.

[15] P. Y. Lau, K. K. O. Yung, and E. K. N. Yung, "A low-cost printed CP patch antenna for RFID smart bookshelf in library," *IEEE Transactions on Industrial Electronics*, vol.57, no.5, pp.1583–1589, 2010.

[16] S. X. Ta, J. J. Han, R. W. Ziolkowski, *et al.*, "Wide-beam circularly polarized composite cavity-backed crossed scythe-shaped dipole," in *Proceedings of the 2013 Asia-Pacific Microwave Conference Proceedings*, Seoul, South Korea, pp.1085–1087, 2013.

[17] K. W. Yang, F. S. Zhang, C. Li, *et al.*, "A wideband planar magneto-electric tapered slot antenna with wide beamwidth," *International Journal of RF and Microwave Computer-Aided Engineering*, vol.29, no.11, article no.e21910, 2019.

[18] Z. S. Duan, S. B. Qu, Y. Wu, *et al.*, "Wide bandwidth and broad beamwidth microstrip patch antenna," *Electronics Letters*, vol.45, no.5, pp.249–251, 2009.

[19] Y. L. Wang, S. Q. Xiao, Y. P. Shang, *et al.*, "A compact and dual-band circularly polarized petal-shaped antenna with broad beamwidth for multiple global navigation satellite systems," in *Proceedings of the 2015 IEEE MTT-S International Microwave Workshop Series on Advanced Materials and Processes for RF and THz Applications*, Suzhou, China, pp.1–3, 2015.

[20] Y. B. Kim, H. J. Dong, K. S. Kim, *et al.*, "Compact planar multipole antenna for scalable wide beamwidth and bandwidth characteristics," *IEEE Transactions on Antennas and Propagation*, vol.68, no.5, pp.3433–3442, 2020.

[21] W. B. Qiu, C. Chen, W. D. Chen, *et al.*, "A planar dipole antenna with parasitic elements for beamwidth enhancement across a wide frequency band," in *Proceedings of the 2017 IEEE International Symposium on Antennas and Propagation & USNC/URSI National Radio Science Meeting*, San Diego, CA, USA, pp.333–334, 2017.

[22] S. Y. Ko and J. H. Lee, "Hybrid zeroth-order resonance patch antenna with broad *E*-plane beamwidth," *IEEE Transactions on Antennas and Propagation*, vol.61, no.1, pp.19–25, 2013.

[23] N. Yang, Z. B. Weng, L. Wang, *et al.*, "A hybrid dual-mode dielectric resonator antenna with wide beamwidth," *International Journal of RF and Microwave Computer-Aided Engineering*, vol.30, no.10, article no.e22337, 2020.

[24] N. W. Liu, S. Gao, L. Zhu, *et al.*, "Low-profile microstrip patch antenna with simultaneous enhanced bandwidth, beamwidth, and cross-polarisation under dual resonance," *IET Microwaves, Antennas & Propagation*, vol.14, no.5, pp.360–365, 2020.

[25] X. Chen, P. Y. Qin, Y. J. Guo, *et al.*, "Low-profile and wide-beamwidth dual-polarized distributed microstrip antenna," *IEEE Access*, vol.5, pp.2272–2280, 2017.

[26] Q. Chen, H. Zhang, and L. H. Xiong, "A dual-patch polarization rotation reflective surface and its application to wideband wide-beam low-profile circularly polarized patch antennas," *International Journal of RF and Microwave Computer-Aided Engineering*, vol.29, no.2, article no.e21533, 2019.

[27] K. Agarwal, Nasimuddin, and A. Alphones, "RIS-based compact circularly polarized microstrip antennas," *IEEE Transactions on Antennas and Propagation*, vol.61, no.2, pp.547–554, 2013.

[28] Q. Chen, H. Zhang, Y. J. Shao, *et al.*, "Bandwidth and gain improvement of an L-Shaped slot antenna with metamaterial loading," *IEEE Antennas and Wireless Propagation Letters*, vol.17, no.8, pp.1411–1415, 2018.

[29] Y. LIU, J. Wang, and S. X. Gong, "Low-profile dual-polarized planar antenna with compact structure for base stations," *Chinese Journal of Electronics*, vol.26, no.5, pp.1092–1095, 2017.

[30] S. Y. Luo, Y. S. Li, T. Jiang, *et al.*, "FSS and meta-material based low mutual coupling MIMO antenna array," in *Proceedings of the 2019 IEEE International Symposium on Antennas and Propagation and USNC-URSI Radio Science Meeting*, Atlanta, GA, USA, pp.725–726, 2019.

[31] C. Shen, W. J. Lu, and L. Zhu, "Planar self-balanced magnetic dipole antenna with wide beamwidth characteristic," *IEEE Transactions on Antennas and Propagation*, vol.67, no.7, pp.4860–4865, 2019.

[32] J. H. Ou, S. W. Dong, J. W. Huang, *et al.*, "A compact microstrip antenna with extended half-power beamwidth and harmonic suppression," *IEEE Transactions on Antennas and Propagation*, vol.68, no.6, pp.4312–4319, 2020.

[33] Y. J. He and Y. Li, "Dual-polarized microstrip antennas with capacitive via fence for wide beamwidth and high isolation," *IEEE Transactions on Antennas and Propagation*, vol.68, no.7, pp.5095–5103, 2020.

[34] Q. Li, W. J. Lu, S. G. Wang, *et al.*, "Planar quasi-isotropic magnetic dipole antenna using fractional-order circular sector cavity resonant mode," *IEEE Access*, vol.5, pp.8515–8525, 2017.

[35] W. J. Lu, X. Q. Li, Q. Li, *et al.*, "Generalized design approach to compact wideband multi-resonant patch antennas," *International Journal of RF and Microwave Computer-Aided Engineering*, vol.28, no.8, article no.e21481, 2018.

[36] W. J. Lu, Q. Li, S. G. Wang, *et al.*, "Design approach to a novel dual-mode wideband circular sector patch antenna," *IEEE Transactions on Antennas and Propagation*, vol.65, no.10, pp.4980–4990, 2017.

[37] J. Yu, W. J. Lu, Y. Cheng, *et al.*, "Tilted circularly polarized beam microstrip antenna with miniaturized circular sector patch under wideband dual-mode resonance," *IEEE Transactions on Antennas and Propagation*, vol.68, no.9, pp.6580–6590, 2020.

[38] X. H. Mao, F. Y. Ji, S. S. Gu, *et al.*, "Circumferentially short-circuited circular sector patch antenna with broadened beamwidth," in *Proceedings of the 2021 IEEE International Symposium on Antennas and Propagation and USNC-URSI Radio Science Meeting*, Singapore, pp.1397–1398, 2021.

[39] W. J. Lu and L. Zhu, "Planar dual-mode wideband antenna using short-circuited-strips loaded slotline radiator: Operation principle, design, and validation," *International Journal of RF and Microwave Computer-Aided Engineering*, vol.25, no.7, pp.573–581, 2015.

[40] W. J. Lu and L. Zhu, "A novel wideband slotline antenna with dual resonances: principle and design approach," *IEEE Antennas and Wireless Propagation Letters*, vol.14, pp.795–798, 2015.

[41] J. Yu and W. J. Lu, "Design approach to dual-resonant, very low-profile circular sector patch antennas," in *Proceedings of the 2019 International Conference on Microwave and Millimeter Wave Technology*, Guangzhou, China, pp.1–3, 2019.

[42] X. Zhang and L. Zhu, "High-gain circularly polarized microstrip patch antenna with loading of shorting pins," *IEEE Transactions on Antennas and Propagation*, vol.64, no.6, pp.2172–2178, 2016.

[43] X. Zhang, L. Zhu, N. W. Liu, *et al.*, "Pin-loaded circularly-polarised patch antenna with sharpened gain roll-off rate and widened 3-dB axial ratio beamwidth," *IET Microwaves, Antennas & Propagation*, vol.12, no.8, pp.1247–1254, 2018.

[44] J. Y. Siddiqui and D. Guha, "Improved formulas for the input impedance of probe-fed circular microstrip antenna," in *Proceedings of the IEEE Antennas and Propagation Society International Symposium. Digest. Held in conjunction with: USNC/CNC/URSI North American Radio Sci. Meeting*, Columbus, OH, USA, pp.152–155, 2003.

[45] H. Wu, W. J. Lu, C. Shen, *et al.*, "Wide beamwidth planar self-balanced magnetic dipole antenna with enhanced front-to-back ratio," *International Journal of RF and Microwave Computer-Aided Engineering*, vol.30, no.5, article

no.e22171, 2020.

[46] Y. Zhang, Z. L. Xue, and W. Hong, "Planar substrate-integrated endfire antenna with wide beamwidth for Q-band applications," *IEEE Antennas and Wireless Propagation Letters*, vol.16, pp.1990–1993, 2017.

MAO Xiaohui was born in Nantong, Jiangsu Province, China, in 1995. She received the B.E. degree in network engineering from Jinling Institute of Technology, Nanjing, China, in 2018. She is currently pursuing the Ph.D. degree with the Nanjing University of Posts and Telecommunications, Nanjing, China. Her recent research interests include the microstrip antennas theory and design approach.
(Email: 2021010101@njupt.edu.cn)

LU Wenjun (corresponding author) was born in Jiangmen, Guangdong Province, China, in 1978. He received Ph.D. degree in electronic engineering from the Nanjing University of Posts and Telecommunications (NUPT), Nanjing, China, in 2007. He has been a Professor with the Jiangsu Key Laboratory of Wireless Communications, NUPT, since 2013. His research interests include antenna theory, antenna design, antenna arrays, and wireless propagation channel modelling. From 2015 to 2016, he invented the design approach to planar endfire circularly polarized antennas. Recently, he has rediscovered the concept of 1-D multi-mode resonant dipoles and advanced the multi-mode resonant design approach to elementary antennas. He is the translator of the Chinese version *The Art and Science of Ultrawideband Antennas* (by H. Schantz). He has authored two books, *Antennas: Concise Theory, Design and Applications* (in Chinese, 2014), and its 2nd edition of *Concise Antennas* (in Chinese, 2020). He has authored or co-authored over 200 technical papers published in peer-reviewed international journals and conference proceedings. He was a recipient of the Exceptional Reviewers Award of the *IEEE Transactions on Antennas and Propagation* in 2016 and 2020, and the Outstanding Reviewers Award of the AEÜ: *Int. J. of Electronics and Communications* in 2018. He has been serving as an Editorial Board Member of the *International Journal of RF and Microwave Computer-Aided Engineering* since 2014, and an Associate Editor of the *Electronics Letters* since 2019. He's a Committee Member of the Antennas Society of Chinese Institute of Electronics (CIE). He's a Senior Member of the CIE and the IEEE.
(Email: wjlu@njupt.edu.cn)

JI Feiyan was born in Taizhou, Jiangsu Province, China, in 1997. She received the B.E. degree in communication engineering from Jiangnan University, Wuxi, China, in 2019. She is currently pursuing the M.E. degree with the Nanjing University of Posts and Telecommunications, Nanjing, China. Her recent research interests include the complementary antennas theory and design approach.
(Email: 1019010127@njupt.edu.cn)

XING Xiuqiong was born in Nanjing, Jiangsu Province, China, in 1994. She received the B.S. degree in electronics and information engineering from Nanjing University of Posts and Telecommunications, Nanjing, China, in 2017. Currently, she is working toward the M.E. degree in Nanjing University of Posts and Telecommunications, Nanjing, China. Her recent research interests include the microtrip antennas theory and design approach.
(Email: 1219012407@njupt.edu.cn)

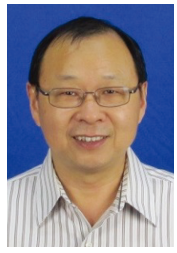

ZHU Lei received the B.E. and M.E. degrees in radio engineering from the Nanjing Institute of Technology (now Southeast University), Nanjing, China, in 1985 and 1988, respectively, and the Ph.D. degree in electronic engineering from the University of Electro-Communications, Tokyo, Japan, in 1993. From 1993 to 1996, he was a Research Engineer with Matsushita-Kotobuki Electronics Industries Ltd., Tokyo, Japan. From 1996 to 2000, he was a Research Fellow with the École Polytechnique de Montréal, Montréal, QC, Canada. From 2000 to 2013, he was an Associate Professor with the School of Electrical and Electronic Engineering, Nanyang Technological University, Singapore. He joined the Faculty of Science and Technology, University of Macau, Macau, China, as a Full Professor in August 2013, and has been a Distinguished Professor since December 2016. From August 2014 to August 2017, he served as the Head of Department of Electrical and Computer Engineering, University of Macau. So far, he has authored or coauthored more than 700 papers in international journals and conference proceedings. His papers have been cited more than 12,500 times with the H-index of 55 (source: Scopus). His research interests include microwave circuits, antennas, periodic structures, and computational electromagnetics.
Dr. Zhu was the Associate Editors for the *IEEE Transactions on Microwave Theory and Techniques* (2010–2013) and *IEEE Microwave and Wireless Components Letters* (2006–2012). He served as a General Chair of the 2008 IEEE MTT-S International Microwave Workshop Series on the Art of Miniaturizing RF and Microwave Passive Components, Chengdu, China, and a Technical Program Committee Co-Chair of the 2009 Asia–Pacific Microwave Conference, Singapore. He served as the Member of IEEE MTT-S Fellow Evaluation Committee (2013–2015), and as the Member of IEEE AP-S Fellows Committee (2015–2017). He was the recipient of the 1997 Asia–Pacific Microwave Prize Award, the 1996 Silver Award of Excellent Invention from Matsushita-Kotobuki Electronics Industries Ltd., the 1993 Achievement Award in Science and Technology (first prize) from the National Education Committee of China, the 2020 FST Research Excellence Award from the University of Macau, and the 2020 Macao Natural Science Award (second prize) from the Science and Technology Development Fund (FDCT), Macau. He is the Fellow of IEEE.
(Email: LeiZhu@um.edu.mo)